Advances in Rheumatology

RESEARCH

Open Access

Morphofunctional analysis of fibroblast-like synoviocytes in human rheumatoid arthritis and mouse collagen-induced arthritis

Camilla Ribeiro Lima Machado[1*], Felipe Ferraz Dias[3], Gustavo Gomes Resende[4], Patrícia Gnieslaw de Oliveira[5], Ricardo Machado Xavier[6], Marcus Vinicius Melo de Andrade[1] and Adriana Maria Kakehasi[2]

Abstract

Background Fibroblast-like synoviocytes (FLS) play a prominent role in rheumatoid synovitis and degradation of the extracellular matrix through the production of inflammatory cytokines and metalloproteinases (MMPs). Since animal models are frequently used for elucidating the disease mechanism and therapeutic development, it is relevant to study the ultrastructural characteristics and functional responses in human and mouse FLS. The objective of the study was to analyze ultrastructural characteristics, Interleukin-6 (IL-6) and Metalloproteinase-3 (MMP-3) production and the activation of intracellular pathways in Fibroblast like synoviocytes (FLS) cultures obtained from patients with rheumatoid arthritis (RA) and from mice with collagen-induced arthritis (CIA).

Methods FLSs were obtained from RA patients (RA-FLSs) (n = 8) and mice with CIA (CIA-FLSs) (n = 4). Morphology was assessed by transmission and scanning electron microscopy. IL-6 and MMP-3 production was measured by ELISA, and activation of intracellular signaling pathways (NF-κB and MAPK: p-ERK1/2, p-P38 and p-JNK) was measured by Western blotting in cultures of RA-FLSs and CIA-FLSs stimulated with tumor necrosis factor-alpha (TNF-α) and IL-1β.

Results RA-FLS and CIA-FLS cultures exhibited rich cytoplasm, rough endoplasmic reticula and prominent and well-developed Golgi complexes. Transmission electron microscopy demonstrated the presence of lamellar bodies, which are cytoplasmic structures related to surfactant production, in FLSs from both sources. Increased levels of pinocytosis and numbers of pinocytotic vesicles were observed in RA-FLSs ($p < 0.05$). Basal production of MMP-3 and IL-6 was present in RA-FLSs and CIA-FLSs. Regarding the production of MMP-3 and IL-6 and the activation of signaling pathways, the present study demonstrated a lower response to IL-1β by CIA-FLSs than by RA-FLSs.

Conclusion This study provides a comprehensive understanding of the biology of RA-FLS and CIA-FLS. The differences and similarities in ultrastructural morphology and important inflammatory cytokines shown, contribute to future in vitro studies using RA-FLS and CIA-FLS, in addition, they indicate that the adoption of CIA-FLS for studies should take careful and be well designed, since they do not completely resemble human diseases.

Keywords Fibroblast-like synoviocytes, Rheumatoid arthritis, Collagen-induced arthritis, Signaling transduction, Interleukin-6, Metalloproteinases, Electronic microscopy

*Correspondence:
Camilla Ribeiro Lima Machado
camillarlmachado@gmail.com
Full list of author information is available at the end of the article

Background

Rheumatoid arthritis (RA) is the most common inflammatory rheumatic disease. Destructive damage of the joints, resulting in physical disability, is the ultimate result of bone and cartilage damage mediated by the production of chemokines and matrix components by synoviocytes [1]. The etiopathogenesis of RA involves an intricate network of cellular interactions in the synovial membrane characterized by the proliferation of cells in the synovial lining, resulting in hyperplasia, pannus formation, and tissue destruction [1, 2].

Fibroblast-like synoviocytes (FLSs) are mesenchymal-derived cells responsible for providing support, nourishment and lubrication to the joint tissue. FLSs one of the most prominent cells in inflamed tissue in RA [2]. In the chronic inflammatory milieu of the rheumatoid synovium, these cells become autonomous, hyperplastic, and invasive and produce large amounts of proinflammatory cytokines, chemokines, and matrix-degrading enzymes [2]. Among these products, metalloproteinases (MMPs) are of fundamental importance in the pathophysiology of RA by promoting bone and cartilage degradation [3, 4] Stromelysin (MMP-3) is one of the most important factors in RA [5, 6]. In addition, FLSs produce interleukin 6 (IL-6), an important cytokine in the inflammatory cascade, leading to the interaction of FLS and other immune cells in the synovium and exacerbating inflammatory processes [7–10]. Previous studies of FLSs from patients with RA indicated that both IL-6 and MMP production increased after IL-1 and TNF-α stimulation and were dependent on the NF-κB and MAPK pathways (ERK, JNK and p38), ultimately contributing to the pathogenesis of RA [11–16].

Animal models have contributed to improved understanding of human disease and provide a useful tool for therapeutic testing. However, the therapies for humans' diseases have developed, they are more precise and specifically targeted, and it becomes gradually important to understand the limitations of generalizing data from mice to humans. Discrepant results from animal and human studies are worrisome, and efforts to evaluate morphological and functional similarities between animal and human cells are required. One of the most commonly used experimental models to study RA is murine collagen-induced arthritis (CIA). This animal model is characterized by peripheral symmetrical joint involvement that shares many histopathological features with human RA, including synovitis, pannus formation, cartilage and bone erosion [17, 18]. Furthermore, as in patients with RA, IL-6 and MMP-3 also play key roles in this model [19–21]. However, we could only find one study showing the effect of IL-1β and TNF-α in FLSs in CIA [20].

Primary FLS cultures from CIA and RA patients have been used as an in vitro exchange model to study the responses of these cells to different stimuli and pharmacological drugs. There have been no studies that exploring the morphological ultrastructures and responses of cultures of FLSs derived from patients with RA (RA-FLS) and mice with CIA (CIA-FLS). Our objective was to investigate RA-FLS and CIA-FLS cultures regarding their ultrastructural characteristics as well as their functional responses, such as the signaling pathways activated and the production of IL-6 and MMP-3 after stimulation with TNF-α and IL-1β.

Methods

Sample collection and culture of RA patient cells

Synovial fluid was obtained from eight (n = 8) RA patients according to the American College of Rheumatology (ACR) criteria [22]. The mean age of the patients was 52.62 years (range 37–66 years). Samples of synovial fluid were collected and centrifuged at 1200 revolutions per minute (rpm) for 10 min. The pellet was resuspended in complete medium (DMEM high glucose plus 10% fetal bovine serum [FBS, Gibco, Life Technologies, USA], 1% streptomycin(S)/penicillin(P) and amphotericin B [Gibco, Life Technologies, USA] and 1% non-essential amino acids [Gibco, Life Technologies, USA]) and kept at 37 °C and 5% CO_2 in cell culture flasks. The culture medium was exchanged every three days until the cells were frozen. FLSs were used for experiments after five passages. The Ethics Committee approved the protocol (CAAE Human Research Ethics Committee: 08387918.6.0000.5149). Informed consent was obtained from all participants in the study.

Sample collection and culture of mouse collagen-induced arthritis cells

Four (n = 4) male DBA1/J mice (8–12 weeks, average weight of 20 g) were used to obtain CIA-FLSs. The animals were immunized with 100 μL of emulsions containing equal parts of Freund's complete adjuvant containing 5 mg/ml heat-killed *Mycobacterium tuberculosis* antigen (strain H37Ra; Difco, Lawrence, USA) and 2 mg/ml type II collagen (Chondrex; Washington, USA) in 10 mM acetic acid on day 0, the administration was by intradermal injection at the base of the tail. The booster was administered after 18 days, consisting of equal parts of Freund's incomplete adjuvant and 2 mg/ml type II collagen in 10 mM acetic acid. Clinical evaluation was performed, the degree of swelling and erythema of the paws, using a standardized method of arthritis scoring, in which 0 = normal, 1 = mild swelling and erythema, 2 = moderate swelling and erythema, 3 = severe swelling and erythema plus loss of function in 2 paws, and 4 = total loss

of function in a minimum of 3 paws. The onset of the disease, characterized by the development of erythema and/or swelling of the paw. After ten days, the animals were sacrificed by cervical dislocation. The synovial tissue was removed from ankle, knee and elbow joints and processed with a 1 mg/ml collagenase solution I (Merck, Saint Louis, USA) for one hour. After centrifugation, the pellet was resuspended in complete medium and cultured in the same way described for human samples until the cells were frozen. FLSs were used for experiments after five passages. All procedures using mice were in accordance with the National Institutes of Health Guide for the Care and Use of Animals. The Animal Use Ethics Committee (Protocol 293/2018) approved the animal study.

Immunophenotyping

RA-FLSs and CIA-FLSs were plated at 2×10^5 cells/well in 20 µl/well and diluted in 20 µl of flow cytometry buffer solution (PBS containing 1% fetal bovine serum and 0.01% azide). For human FLSs, anti-human CD14 PerCP-Cyanine 5.5 (ref. 45-0149, eBioscience), anti-human CD45 V450 (ref. 560368, BD Biosciences), and anti-human CD90 Phycoerythrin (PE) (ref. 561,970, BD Biosciences) monoclonal antibodies and V450-, PE- and PerCP-labeled isotype control antibodies were used (all from BD Biosciences), and unlabeled control cells were included in all experiments. For mouse FLSs, anti-mouse CD45 V450 (ref. 19264, BD Biosciences) and anti-rat CD90.1 PE (ref. 554898, BD Biosciences) monoclonal antibodies, V450- and PE-labeled isotype control antibodies (all BD Biosciences) and unlabeled cells were used. Cells were labeled with antibodies for 20 min at 4 °C in the dark, washed, resuspended in 1 × PBS and analyzed on a FACSCanto II flow cytometer (BD Biosciences). A minimum of 100,000 events were acquired for each sample, and the acquisitions were processed using Diva software (BD Biosciences). FlowJo software (Tree Star) was used to analyze the data.

Electron microscopy

Morphological analysis was performed by scanning electron microscopy (SEM) and transmission electron microscopy (TEM). For SEM, RA-FLSs and CIA-FLSs were cultured without stimulation on poly-L-lysine-treated coverslips. After cell fixation, the media was aspirated, and the cells were washed with 1 × saline phosphate buffer (SPB). The cultures were then immersed in 2.5% glutaraldehyde in 0.1 M cacodylate buffer. After 120 min, the fixation solution was aspirated and replaced with 0.1 M cacodylate buffer. The samples were washed in aldehyde three times for 10 min each in 0.05 M cacodylate buffer and immersed in 1% osmium tetraoxide (OsO4) solution in 0.05 M cacodylate buffer for one hour at room temperature. The samples were washed in distilled water and dehydrated with increasing concentrations of alcohol (30, 50, 70, 90 and 100%) and acetone for 10 min each. The dehydrated samples were dried until the acetone was completely removed. The samples were visualized by SEM (FEG-Quanta 200 FEI). Cell shape, the emission of cytoplasmic projections, and the presence of filopodia and lamellipodia were analyzed in 20 RA-FLSs and 20 CIA-FLSs.

For TEM analysis of unstimulated RA-FLS and CIA-FLS, the preparation included aspiration of DMEM followed by washes with SPB. The cultures were then fixed for 120 min with 2.5% glutaraldehyde in 0.1 M cacodylate buffer at 4 °C. The fixed samples were scraped off with a spatula, transferred to sterile 50 ml tubes and centrifuged at 3000 rpm for 5 min. The pellets were fixed in 2% osmium tetroxide (Sigma-Aldrich, Sao Paulo, Brazil) in 0.1 M cacodylate buffer for 2 h at room temperature. After being washed three times with distilled water for 15 min each, the samples were incubated with 2% uranyl acetate (EMS) for 24 h at room temperature in the dark. The samples were then washed with distilled water as described above and dehydrated in an increasing series of alcohol (35, 50, 70, 85, 95, and 100%) and acetone for 20 min each. After dehydration, infiltration was followed by incubation in a 1:2, 1:1 and 1:2 mixture of acetone-Epon resin (EMBed Resin 812, EMS) and pure resin for 3 h. Subsequently, the cells were incubated in the same resin in BEEM capsules (Ted Pella, California, USA) and polymerized at 60 °C for 48 h. After polymerization of the resin, 300 nm semifine sections were obtained from the surface of the blocks with the aid of glass razors and stained with toluidine-sodium borate blue. Ultrathin sections (~60 nm) were obtained on a Leica EM UC6 ultramicrotome (Leica Microsystems GmbH, Wetzlar, Germany) using a diamond razor. The sections were mounted on 200 mesh copper (Ted Pella), stained with lead citrate (Merck KGaA, Darmstadt, Germany) for 5 min and analyzed under a transmission electron microscope (Tecnai G2-12 Spirit Biotwin Thermo Fischer Scientific/FEI 2006, Eindhoven, the Netherlands) at 120 kV. Cells were visualized by MET (Tecnai G2-12 Spirit Biotwin FEI - 120 kV).

To investigate the morphological characteristics of synoviocytes, images of 20 cells per group revealing the entire cellular profile, including the nucleus, and subcellular details were obtained at 4200-fold, 16,500-fold and 20,500-fold magnifications. The basic ultrastructural analyses focused on organelles involved with the classic cell synthesis and secretion pathway: the nucleus (N), rough endoplasmic reticulum (RER), Golgi apparatus

(GA) and mitochondria (MT). The morphometric analyses were focused on organelles involved in cellular pinocytosis (pinocytosis (P) and pinocytic vesicles (PV)), lamellar bodies (LBs) and MT. The morphometric analysis was based on the relative quantity of each organelle per number of cells.

Stimuli and treatments

RA-FLSs and CIA-FLSs were plated in 24-well plates (1.5×10^5 cells/well) in DMEM with 1% P/S/amphotericin B and 1% FBS for 24 h at 37 °C in 5% CO2. The cells were then stimulated for 24 h with 50 ng/ml TNF-α (ref.: human 300-01A and murine 315-01A, Peprotech) and 1 ng/ml IL-1β (ref.: human 200-01B and murine 211-11B, Peprotech).

After stimulation, the supernatant was used to measure the production of IL-6 and MMP-3 by ELISA (R&D Systems) according to the manufacturer's protocols. For signaling pathway analysis, both cell types were transferred to six-well plates (1 X 10^6 cells/well) and stimulated with 50 ng/ml TNF-α and 1 ng/ml IL-1β for 30 min. After stimulation, the cells were lysed. The cell lysate buffer contained 25 mM Tris–HCl, pH 7.5, 150 mM NaCl, 1% Nonidet P-40, 5 mM sodium pyrophosphate, 1 mM sodium orthovanadate, 10 mM sodium fluoride, 10% glycerin, 1 mM phenylmethylsulfonyl fluoride and 1 protease inhibitor cocktail set I (Calbiochem, California, USA). The following phosphorylated proteins in the cell lysate were analyzed: ERK1/2 (ref: 9101, Cell Signaling), p38 (ref: 4511, Cell Signaling), and JNK (ref: 9251, Cell Signaling), and the transcription factors NF-κB (ref: 3033, Cell Signaling) and β-actin (ref: ARG53987, Arigo) were analyzed.

Statistical analysis

The Mann–Whitney U test nonparametric analysis was used to compare MMP-3 and IL-6 concentrations between the TNF-α- and IL-1β-stimulated groups and to compare the amounts of pinocytosis, pinocytic vesicles, mitochondria, and lamellar bodies between RA-FLSs and CIA-FLSs. GraphPad Prisma version 6.01 was used for data analysis and graph production. We considered evidence of significant effects at p-values < 0.05.

Results

Immunophenotyping

RA-FLSs and CIA-FLSs were positive for the FLS marker CD90 (Fig. 1A–C). RA-FLSs were negative for the leukocyte marker CD45 and the monocyte/macrophage marker CD14 (Fig. 1A, B). In CIA-FLSs, controls for leukocyte markers (CD45) also demonstrated the presence of a pure FLS culture (< 1% CD45+) (Fig. 1D).

Scanning electron microscopy

RA-FLS and CIA-FLS cultures exhibited populations of fusiform FLSs with cytoplasmic expansions forming branches. Both cell types were anchored to the substrate with numerous cytoplasmic projections at the lamellipodia ends, and the protein structure of the actin cytoskeleton protruded at the mobile end of the cell [23]. Lamellipodia propelled entire cell structures through the substrate (Fig. 2).

The cytoplasmic projections that extended beyond the lamellipodia border on migrating cells were often anchored to neighboring cells (Fig. 2).

Transmission electron microscopy

Evaluation of RA-FLSs and CIA-FLSs by Transmission Electron Microscopy (TEM) revealed subcellular characteristics of intense cellular activity, represented by a large and euchromatic nucleus with a thin layer of heterochromatin, a prominent and well-developed rough endoplasmic reticulum and Golgi apparatus, and the presence of several mitochondria close to these organelles (Fig. 3). As shown in Fig. 4, we observed a high concentration of intermediate filaments, which are filamentous protein structures that make up the cytoskeleton of cells and assist in cell morphology. Ultrastructural differences were observed between RA-FLSs and CIA-FLSs in the degree of pinocytosis (number of plasma membrane invaginations) and the number of pinocytotic vesicles, which were related to the process of cellular pinocytosis. Both structures were more frequently seen in RA-FLSs than in CIA-FLSs ($p < 0.05$) (Fig. 4). No significant difference was observed in the number of mitochondria (data not shown).

Lamellar bodies were observed in RA-FLS and CIA-FLS cultures (Fig. 3). Lamellar bodies consist of cavitary structures with circular walls in unique juxtaposition to FLSs in the synovial environment; these structures are secreted by exocytosis in the synovial fluid and secrete hyaluronic acid and surfactant (proteins and lipids) [24]. Lamellar bodies at various stages of maturation were identified in the same cell (Fig. 3C). No significant difference was observed in the number of lamellar bodies between RA-FLSs and CIA-FLSs (data not shown). Adjacent FLSs were observed to be in close contact through their cytoplasmic projections, corresponding to the electron-dense regions at the communication/adherent junction sites.

Functional analysis

Figure 5 shows the activation of MAPK and p-NF-κB signaling in RA-FLSs and CIA-FLSs after stimulation with TNF-α and IL-1β. In RA-FLSs and CIA-FLSs, TNF-α showed a trend to activate p-ERK1/2 (2.25-fold

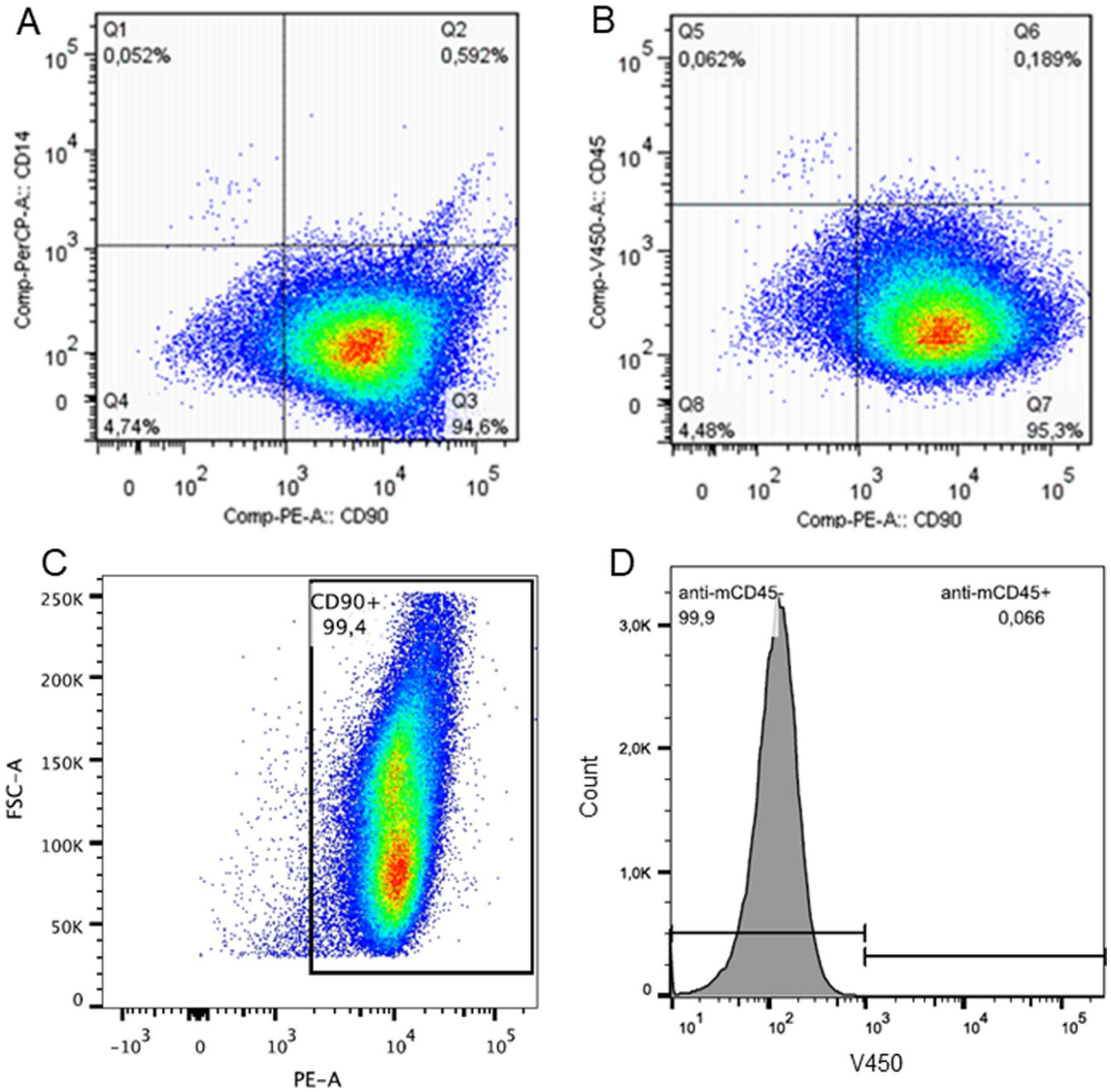

Fig. 1 Immunophenotyping of fibroblast-like synoviocyte cultures from patients with rheumatoid arthritis and mice with collagen-induced arthritis was verified by flow cytometry assays. (A-B) Cell cultures from RA patients were stained with the surface markers CD90, CD14 and CD45. **A** CD90 + CD14− and **B** CD90 + CD45−; **C**, **D** Cell cultures from mice with collagen-induced arthritis were stained with the surface markers CD90 and CD45. **C** CD90 + and **D** CD45−

and 2.44-fold, respectively), p-NF-κB (3.91-fold and 1.18-fold, respectively) and p-P38 (1.48-fold and 4.89-fold, respectively), and TNF-α significantly activated p-JNK (8.53-fold) only in RA-FLS. On the other hand, IL-1β significantly activated p-P38, p-NFκB, p-ERK1/2 and p-JNK (56.06-fold, 35.96-fold, 11.96-fold and 142.31-fold, respectively) in RA-FLSs. In CIA-FLS, IL-1β did not show considerable effect (Fig. 5).

Similarly, MMP-3 and IL-6 (Fig. 6) were constitutively expressed by RA-FLSs and CIA-FLSs even when the cells were unstimulated. In RA-FLSs, significant increases in IL-6 and MMP-3 production were observed after stimulation with TNF-α and IL-1β ($p = 0.0267$; $p = 0.0405$; $p = 0.0405$ and $p = 0.0075$, respectively) (Fig. 6A, B)). However, in CIA-FLSs, there was an increase in IL-6 production only after TNF-α stimulation ($p = 0.0026$). No difference in MMP-3 production after TNF-α stimulation or IL-6 or MMP-3 after IL-1β stimulation (Fig. 6C, D) was detected.

Discussion

Many in vitro studies use cells from experimental models to study the etiopathogenesis of RA [25]. FLSs from experimental models are frequently used in the search of

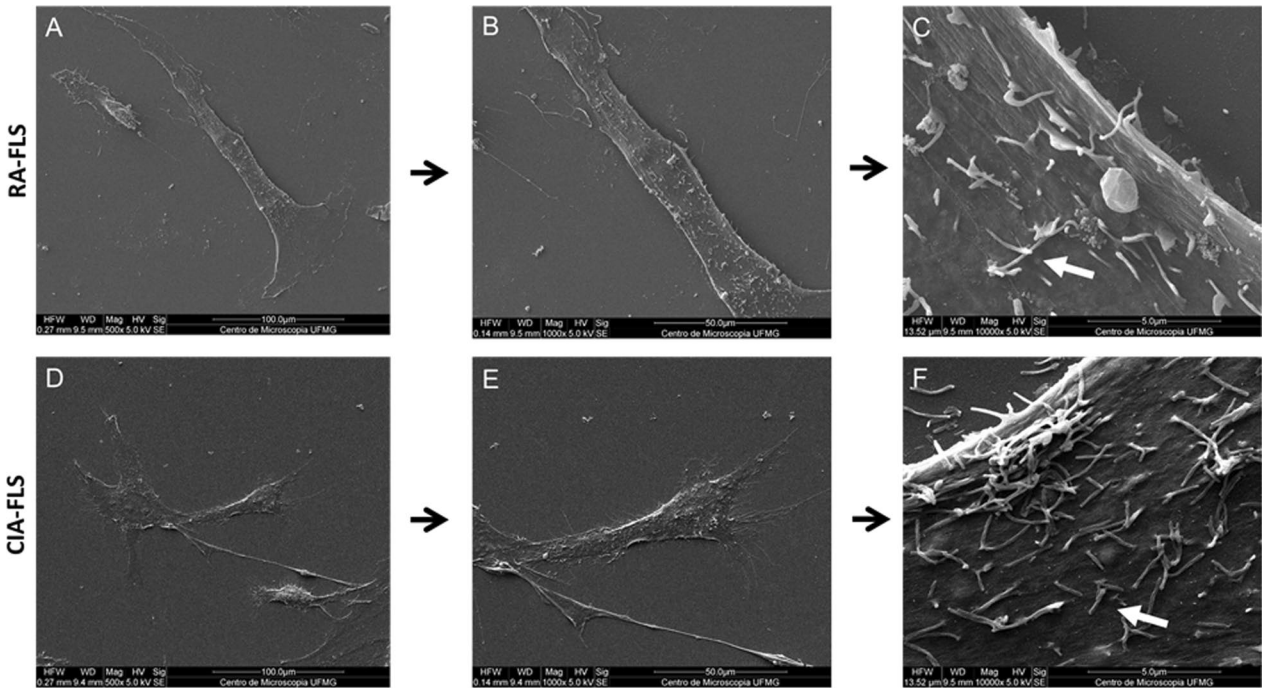

Fig. 2 Fibroblast-like synoviocytes were observed by scanning electron microscopy. **A**–**C** Fibroblast-like synoviocytes from patients with rheumatoid arthritis showing cytoplasmic extensions and the presence of filopodia (white arrow). **D**–**F** Fibroblast-like synoviocytes from mice with collagen-induced arthritis showing the presence of filopodia (white arrow)

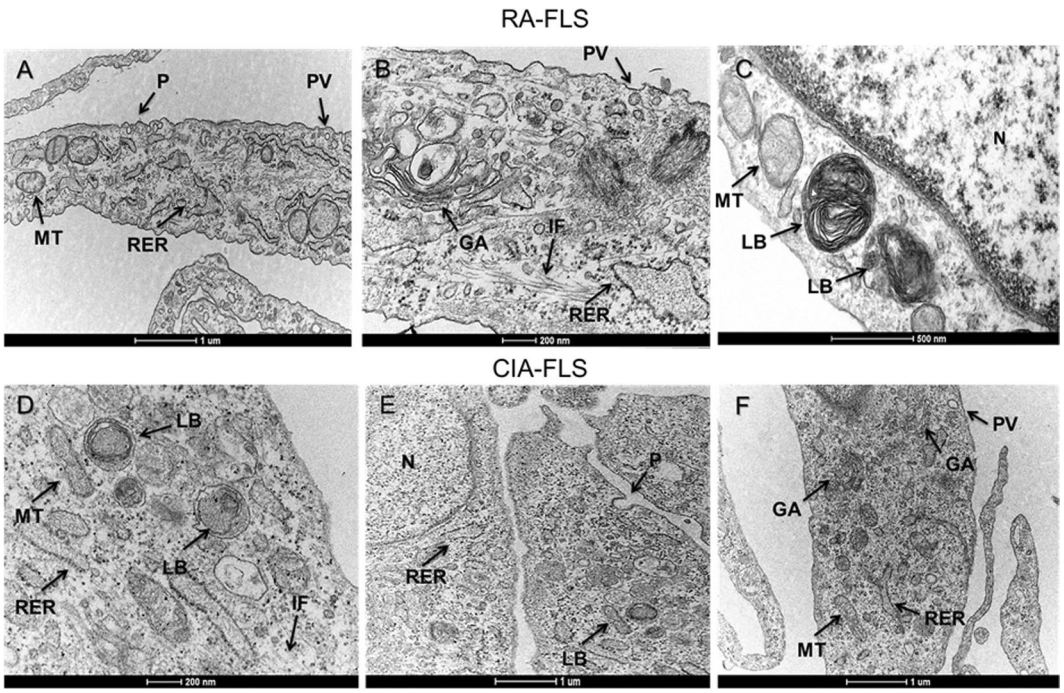

Fig. 3 Electron microscopic analysis of fibroblast-like synoviocytes from patients with rheumatoid arthritis (**A**–**C**) and mice with collagen-induced arthritis (**D**–**F**). Both groups showed an abundant cytoplasm containing mitochondria (MT) with extensive rough endoplasmic reticulum (RER), with an euchromatic nucleus (N), mitochondria (MT), Golgi apparatus (GA), intermediate filaments (IF), lamellar bodies (LB) showing typical concentric walls, and pinocytotic vesicle (PV) in the cell membrane, showing the presence of pinocytosis (P). (4200-fold, 16,500-fold and 20,500-fold magnifications were used)

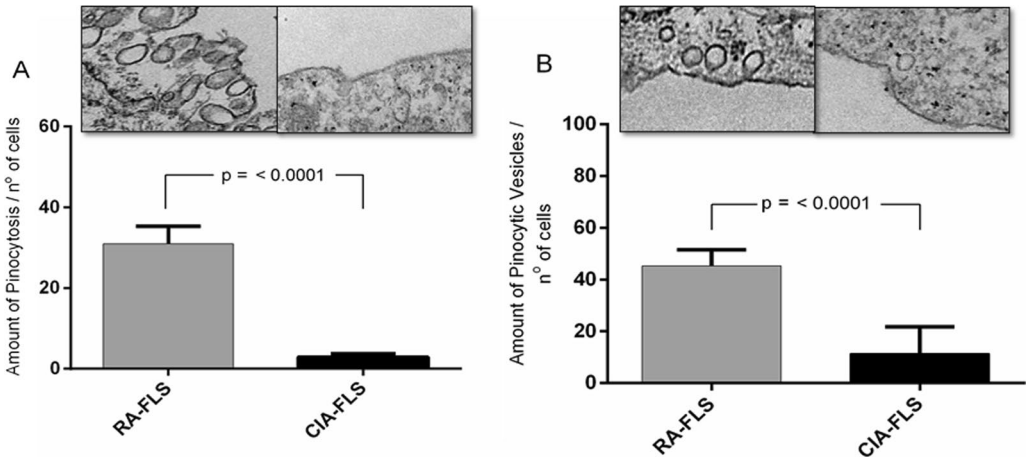

Fig. 4 Pinocytosis vesicle and pinocytosis in fibroblast-like synoviocytes from patients with rheumatoid arthritis (RA-FLS) and mice with collagen-induced arthritis (CIA-FLSs). **A** Higher amount of pinocytosis in RA-FLSs than in CIA-FLSs. **B** Higher numbers of pinocytic vesicles in RA-FLSs than in CIA-FLSs. $p < 0.05$ was considered statistically significant

therapeutic targets and to study the effects of new drugs, and it is well established that FLSs play important roles in cartilage and bone destruction in the joints of patients with RA [2]. Previous study has shown that histopathological and pathological characteristics in the inflamed tissues of mice with CIA and patients with RA are similar [26]. However, the present study showed ultrastructural differences, differences in the production of important mediators of inflammation in RA, and different signaling pathways were activated between human- and mouse-derived FLSs in vitro. Our group showed previously the similarity of FLS derived from synovial tissue and FLS derived from synovial fluid, which explains the use of RA-FLS from synovial fluid and CIA-FLS from tissue fluid in this study [27]. Furthermore, it was a limitation of the study has only FLS from experimental models in an established phase of the disease, however, this places these cells at the same time as RA-FLS, in which the disease is already established and not in the early stage.

In accordance with our data, we found important morphological differences between RA-FLS and CIA-FLS. Our data demonstrate for the first time a higher degree of pinocytosis and more pinocytotic vesicles in human cells than in mouse cells. Pinocytosis, a type of endocytosis, plays a critical role in cell transport, endocytosis, signal transduction, and cell proliferation [28–30]. When endocytosis occurs, the cell extends and folds around the extracellular material, forming a pocket and then creating pinocytic vesicles that are absorbed [31, 32]. Therefore, these morphological differences could indicate increased functional activity in RA-FLSs.

Despite these differences, many similarities between RA-FLS and CIA-FLS morphology were observed, including the presence of lamellar bodies, fusiform shape, the presence of lamellipodia, large euchromatic nucleus, prominent and well-developed rough endoplasmic reticulum and Golgi apparatus, and the presence of several mitochondria nearby to these organelles [24].

Upregulation of IL-6 and MMP-3 after in vitro stimulation with TNF-α and IL-1β in RA-FLS has been previously demonstrated [20, 33, 34]. This stimulation was mediated by activation of the MAPK pathways (ERK, p38 and JNK), as well as the transcription factor NF-κB, and was supported by the findings of other studies [5, 14, 15, 35–42]. Unlike RA-FLSs, in CIA-FLS, after IL-1β stimulation, there was a lack of activation of the MAPK pathways and NF-κB and, consequently, the absence of an increase in the production of IL-6 and MMP-3. Although IL-1β is presented on the inflamed synovium in CIA [43, 44], few studies have demonstrated the expression of the

(See figure on next page.)

Fig. 5 Effect of TNF-α and IL-1β on the activation of the MAP kinase (p-ERK1/2, p-P38, and p-JNK) pathway and the transcription factor NF-κB in Fibroblast-like synoviocytes from patients with rheumatoid arthritis (RA-FLSs) and mice with collagen-induced arthritis (CIA-FLSs). RA-FLS and CIA-FLS were stimulated for 30 min with TNF-α and IL-1β. β-actin and phosphorylated proteins p38, ERK1/2, JNK and NF-κB expression levels were examined by western blotting. **A**–**D** The phosphorylated proteins ERK1/2, p38, JNK and NF-κB in RA-FLS. **E**–**G** The phosphorylated proteins ERK1/2, p38 and NF-κB in CIA-FLS. **H** Representative western blot figure. (Kruskal–Wallis one-way test, $p < 0.05$) NS = unstimulated, TNF-α = tumor necrosis factor alpha, IL-1 beta = interleukin 1 beta

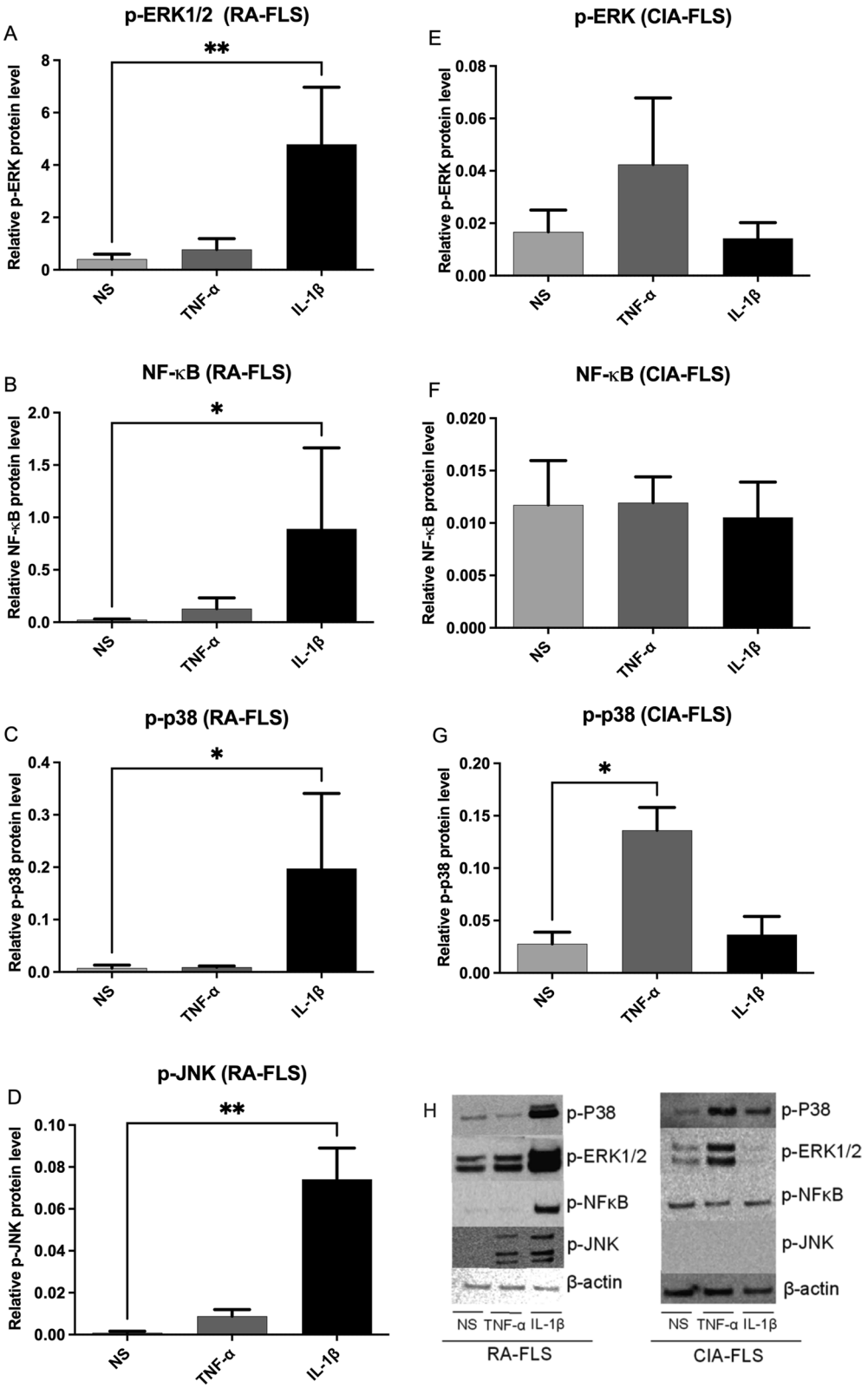

Fig. 5 (See legend on previous page.)

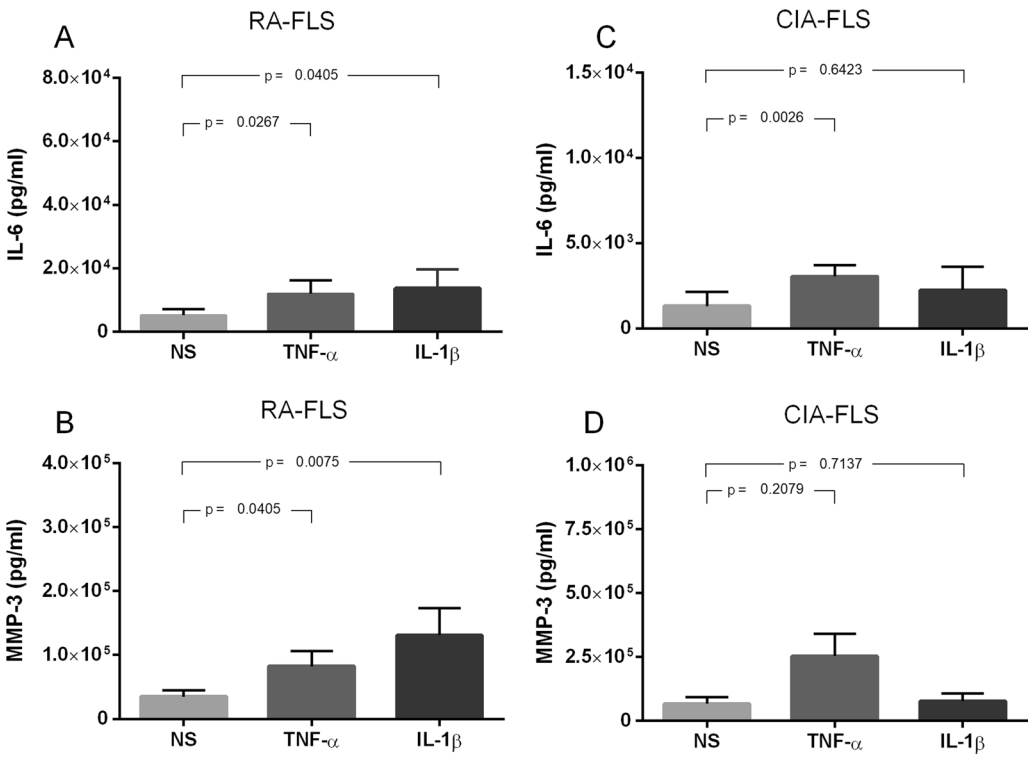

Fig. 6 Production of MMP-3 and IL-6 in response to TNF-α and IL-1β stimulation. Fibroblast-like synoviocytes obtained from patients with rheumatoid arthritis (**A**) and (**B**) (n = 4) and from mice with collagen-induced arthritis (CIA-FLSs) (C) and (D) (n = 4). $P < 0.05$ was considered statistically significant. NS = nonstimulated, TNF-α = tumor necrosis factor alpha, IL-1 = interleukin 1 beta, IL-6 = interleukin 6, MMP-3 = metalloproteinase 3

IL-1β receptor (IL1r1) in CIA-FLSs [42]. The low expression of the IL-1β receptor in CIA-FLSs could explain the lack of activation of downstream signaling pathways and the lack of an increase in MMP-3 and IL-6 production [45]. However, IL-6 production has been observed after IL-1β stimulation in CIA-FLSs [45], but the researchers did not analyze the activation of the signaling pathways that was reported in our work. Our results suggest that the low activation and nonactivation of signaling pathways (p-ERK, p-p38, p-JNK and NF-κB transcription factor) was consistent with the lack of production of MMP-3 and IL-6 [46].

Furthermore, TNF-α plays a major role in the pathogenesis of RA, as well as in CIA [2, 44, 47, 48]. Both groups of cells responded to TNF-α stimulation by activation of the p-ERK, p-p38 and p-NF-κB signaling pathways. These activations mediate an increase in IL-6 production, but only JNK was not phosphorylated in CIA-FLSs. Despite studies showing the activation of this pathway in CIA-FLSs [43], we demonstrated that MMP-3 production was insignificant, which was consistent with the lack of activation of p-JNK [38, 41]. It is possible that MMP-3 does not play as important a role in CIA as it does in RA patients [6, 36, 49]. Therefore, further studies will need to show the differences and similarities between RA-FLS and CIA-FLS.

Conclusion

Experimental models, play an important role in the study of disease mechanisms and the search for possible treatments. It is hard to draw conclusions about the significance of differences between mouse and human biology, however, despite the benefits these models bring, they must be interpreted with care since they do not completely resemble human diseases. Regarding the ultrastructural morphology and important inflammatory cytokines involved in the pathophysiology of RA responses, our study shows where some differences and similarities occur between RA-FLS and CIA-FLS, this could help in future studies using in vitro FLS, and also demonstrate that a well interpretation must be applied in using CIA-FLSs to design in vitro studies related to etiopathogenesis and new therapeutic targets in RA.

Abbreviations

FLS	Fibroblasts like synoviocytes
RA	Rheumatoid arthritis
CIA	Collagen-induced arthritis
IL	Interleukin
MMP	Metalloproteinase
TNF	Tumor necrosis factor
ACR	American College of Rheumatology
RPM	Revolutions per minute
PE	Phycoerythrin
SEM	Scanning electron microscopy
TEM	Transmission electron microscopy
SPB	Saline phosphate buffer
EMS	Uranyl acetate
N	Nucleus
RER	Rough endoplasmic reticulum
GA	Golgi apparatus
MT	Mitochondria
P	Pinocytosis
PV	Pinocytic vesicles
LBs	Lamellar bodies

Author contributions

AMK, MVMA, CRLM conceived and designed the experiments. CRLM performed the experiments and analyzed data. CRLM, FFD, PGO, GGR contributed to acquisition and interpretation of the data. Contributed reagents/materials/analysis tools: MVMA, AMK, RMX. AMK and MVMA supervised the project. All authors read and approved the final manuscript.

Funding

This study received support from Fundo de Apoio à Pesquisa e Ensino—Sociedade Brasileira de Reumatologia (FAPE-SBR), Fundação de Amparo à Pesquisa de Minas Gerais (FAPEMIG), and Conselho Nacional de Desenvolvimento Tecnológico (CNPq).

Availability of data and materials

We will provide all data and materials if needed.

Declarations

Ethical approval and consent to participate

This study was approved by Federal University of Minas Gerais Human Research Ethics Committee and Animal Use Ethics Committee. All the participants gave written informed consent.

Consent for publication

The submission was agreed by all the authors and none of the authors has any potential financial conflict of interest related to this manuscript.

Competing interests

The authors declare no competing interests.

Author details

[1]Laboratory of Scientific Research - Professor Lineu Freire-Maia, Faculty of Medicine, Universidade Federal de Minas Gerais, Belo Horizonte, Brazil. [2]Post Graduate Program in Sciences Applied to Adult Health Care, Universidade Federal de Minas Gerais, Belo Horizonte, Brazil. [3]Laboratory of Scientific Research, Institute of Biological Sciences, Universidade Federal de Minas Gerais, Belo Horizonte, Brazil. [4]Hospital das Clínicas, Universidade Federal de Minas Gerais, Belo Horizonte, Brazil. [5]Medicine Department, University of California of San Diego, San Diego, USA. [6]Internal Medicine Department, Faculty of Medicine, Universidade Federal do Rio Grande do Sul, Porto Alegre, Brazil.

Received: 15 July 2022 Accepted: 28 November 2022
Published online: 03 January 2023

References

1. McInnes IB, Schett G. The pathogenesis of rheumatoid arthritis. N Engl J Med. 2011;365:2205–19.
2. Tu J, Hong W, Zhang P, Wang X, Korner H, Wei W. Ontology and function of fibroblast-like and macrophage-like synoviocytes: how do they talk to each other and can they be targeted for rheumatoid arthritis therapy? Front Immunol. 2018;9:1467.
3. Croft AP, Naylor AJ, Marshall JL, Hardie DL, Zimmermann B, Turner J, Desanti G, Adams H, Yemm AI, Muller-Ladner U, Dayer JM, Neumann E, Filer A. Buckley CD : rheumatoid synovial fibroblasts differentiate into distinct subsets in the presence of cytokines and cartilage. Arthritis Res Ther. 2016;18(1):270.
4. Ekwall AKH, Eisler T, Anderberg C, Jin C, Karlsson N, Brisslert M, Bokarewa MI. The tumour-associated glycoprotein podoplanin is expressed in fibroblast-like synoviocytes of the hyperplastic synovial lining layer in rheumatoid arthritis. Arthritis Res Ther. 2011;13:40.
5. Hammaker DR, Boyle DL, Chabaud-Riou M, Firestein GS. Regulation of c-Jun N-terminal kinase by MEKK-2 and mitogen-activated protein kinase kinase kinases in rheumatoid arthritis. J Immunol. 2004;172:1612–8.
6. Sugiyama E. Role of matrix metalloproteinase-3 in joint destruction in rheumatoid arthritis. Clin Calcium. 2007;17:528–34.
7. Jiao Z, Wang W, Ma J, Wang S, Su Z, Xu H: Notch signaling mediates TNF-α-induced IL-6 production in cultured fibroblast-like synoviocytes from rheumatoid arthritis. Clin Dev Immunol. 2012.
8. Migita K, Iwanaga N, Izumi Y, Kawahara C, Kumagai K, Nakamura T, Koga T, Kawakami A. TNF-α-induced miR-155 regulates IL-6 signaling in rheumatoid synovial fibroblasts. BMC Res Notes. 2017;10:403.
9. Mor A, Abramson SB, Pillinger MH. The fibroblast-like synovial cell in rheumatoid arthritis: a key player in inflammation and joint destruction. Clin Immunol. 2005;115:118–28.
10. Tran CN, Lundy SK, White PT, Endres JL, Motyl CD, Gupta R, Wilke C, Shelden E, Chung K, Urquhart A, Fox D. Molecular interactions between T cells and fibroblast-like synoviocytes: role of membrane tumor necrosis factor-alpha on cytokine-activated T cells. Am J Pathol. 2007;171:1588–98.
11. Bucala R, Ritchlin C, Winchester R, Cerami A. Constitutive production of inflammatory and mitogenic cytokines by rheumatoid synovial fibroblasts. J Exp Med. 1991;173:569–74.
12. Neumann E, Lefevre S, Zimmermann B, Gay S, Muller-Ladner U. Rheumatoid arthritis progression mediated by activated synovial fibroblasts. Trends Mol Med. 2010;16:458–68.
13. Perlman H, Bradley K, Liu H, Cole S, Shamiyeh E, Smith RC, Walsh K, Fiore S, Koch AE, Firestein GS, Haines GK, Pope RM. IL-6 and matrix metalloproteinase-1 are regulated by the cyclin-dependent kinase inhibitor p21 in synovial fibroblasts. J Immunol. 2003;170:838–45.
14. Sweeney SE, Firestein GS. Mitogen activated protein kinase inhibitors: where are we now and where are we going? Ann Rheum Dis. 2006;65:83.
15. Thalhamer T, McGrath MA, Harnett MM. MAPKs and their relevance to arthritis and inflammation. Rheumatology (Oxford). 2008;47:409–14.
16. Rosengren S, Corr M, Boyle DL. Platelet-derived growth factor and transforming growth factor beta synergistically potentiate inflammatory mediator synthesis by fibroblast-like synoviocytes. Arthritis Res Ther. 2010;12:R65.
17. Courtenay JS, Dallman MJ, Dayan AD, Martin A, Mosedale B. Immunisation against heterologous type II collagen induces arthritis in mice. Nat. 1980;283:666–8.
18. Holmdahl R, Andersson M, Goldschmidt TJ, Gustafsson K, Jansson L, Mo JA. Type II collagen autoimmunity in animals and provocations leading to arthritis. Immunol Rev. 1990;118:193–232.
19. Inoue T, Kohno M, Nagahara H, Murakami K, Sagawa T, Kasahara A, Kaneshita S, Kida T, Fujioka K, Wada M, Nakada H, Hla T, Kawahito Y. Upregulation of sphingosine-1-phosphate receptor 3 on fibroblast-like synoviocytes is associated with the development of collagen-induced arthritis via increased interleukin-6 production. PLoS ONE. 2019;14(6):e0218090.
20. Lee A, Choi S-J, Park K, Park JW, Kim K, Choi K, Yoon S-Y, Youn I. Detection of active matrix metalloproteinase-3 in serum and fibroblast-like synoviocytes of collagen-induced arthritis mice. Bioconjug Chem. 2013;24:1068–74.
21. Zhai T, Gao C, Huo R, Sheng H, Sun S, Xie J, He Y, Gao H, Li H, Zhang H, Li H, Sun Y, Lin J, Shen B, Xiao L, Li N. Cyr61 participates in the pathogenesis

of rheumatoid arthritis via promoting MMP-3 expression by fibroblast-like synoviocytes. Mod Rheumatol. 2017;27:466–75.
22. Arnett FC, Edworthy SM, Bloch DA, McShane DJ, Fries JF, Cooper NS, Healy LA, Kaplan SR, Liang MH, Luthra HS, Medsger TA, Mitchell DM, Neustadt DH, Pinals RS, Schaller JG, Sharp JT, Wilder RL, Hunder GG. The American Rheumatism Association 1987 revised criteria for the classification of rheumatoid arthritis. Arthritis Rheum. 1988;31:315–24.
23. Vuorio E, Takala I, Pulkki K, Einola S. Effects of sodium aurothiomalate on hyaluronic acid synthesis in normal and rheumatoid synovial fibroblast cultures. Taylor Francis. 2009;8:173–6.
24. Vandenabeele F, De Bari C, Moreels M, Lambrichts I, Dell'Accio F, Lippens PL, Luyten FP. Morphological and immunocytochemical characterization of cultured fibroblast-like cells derived from adult human synovial membrane. Arch Histol Cytol. 2003;66:145–53.
25. Hu Y, Cheng W, Cai W, Yue Y, Li J, Zhang P. Advances in research on animal models of rheumatoid arthritis. Clin Rheumatol. 2013;32:161–5.
26. Jia Q, Wang T, Wang X, Xu H, Liu Y, Wang Y, Shi Q, Liang Q. Astragalin suppresses inflammatory responses and bone destruction in mice with collagen-induced arthritis and in human fibroblast-like synoviocytes. Front Pharmacol. 2019;10:94.
27. Machado CRL, Resende GG, Macedo RBV, de Nascimento VC, Branco AS, Kakehasi AM, Andrade MV. Fibroblast-like synoviocytes from fluid and synovial membrane from primary osteoarthritis demonstrate similar production of interleukin 6, and metalloproteinases 1 and 3. Clin Exp Rheumatol. 2019;37:306–9.
28. Panariti A, Miserocchi G, Rivolta I. The effect of nanoparticle uptake on cellular behavior: disrupting or enabling functions? Nanotechnol Sci Appl. 2012;5:87.
29. Sinha B, Koster D, Ruez R, Gonnord P, Bastiani M, Abankwa D, Stan RV, Butler-Browne G, Vedie B, Johannes L, Morone N, Parton RG, Raposo G, Sens P, Lamaze C, Nassoy P. Cells respond to mechanical stress by rapid disassembly of caveolae. Cell. 2011;144:402–13.
30. Soldati T, Schliwa M. Powering membrane traffic in endocytosis and recycling. Nat Rev Mol Cell Biol. 2006;7:897–908.
31. Singer II. Microfilament bundles and the control of pinocytotic vesicle distribution at the surfaces of normal and transformed fibroblasts. Exp Cell Res. 1979;122:251–64.
32. Stillwell W. An introduction to biological membranes. Indianapolis: ScienceDirect; 2016. p. 446–7.
33. Bartok B, Firestein GS. Fibroblast-like synoviocytes: key effector cells in rheumatoid arthritis. Immunol Rev. 2010;233:233–55.
34. Baumann H, Kushner I. Production of interleukin-6 by synovial fibroblasts in rheumatoid arthritis. Am J Pathol. 1998;152:641.
35. Bottini N, Firestein GS. Duality of fibroblast-like synoviocytes in RA: passive responders and imprinted aggressors. Nat Rev Rheumatol. 2013;9:24–33.
36. Hammaker D, Sweeney S, Firestein G. Signal transduction networks in rheumatoid arthritis. Ann Rheum Dis. 2003;62:86.
37. Görtz B, Hayer S, Tuerck B, Zwerina J, Smolen JS, Schett G. Tumour necrosis factor activates the mitogen-activated protein kinases p38α and ERK in the synovial membrane in vivo. Arthritis Res Ther. 2005;7:1–8.
38. Han Z, Boyle DL, Chang L, Bennett B, Karin M, Yang L, Manning AM, Firestein GS. c-Jun N-terminal kinase is required for metalloproteinase expression and joint destruction in inflammatory arthritis. J Clin Invest. 2001;108:73–81.
39. Kaneko M, Tomita T, Nakase T, Ohsawa Y, Seki H, Takeuchi E, Takano H, Shi K, Takahi K, Kominami E, Uchiyama Y, Yoshikawa H, Ochi T. Expression of proteinases and inflammatory cytokines in subchondral bone regions in the destructive joint of rheumatoid arthritis. Rheumatology (Oxford). 2001;40:247–55.
40. Lu H, Sun T, Yao L, Zhang Y. Role of protein tyrosine kinase in IL-1 beta induced activation of mitogen-activated protein kinase in fibroblast-like synoviocytes of rheumatoid arthritis. Chin Med J. 2000;113:872–6.
41. Re S. BM F: Signalling, inflammation and arthritis: NF-kappaB and its relevance to arthritis and inflammation. Rheumatology (Oxford). 2008;47:584–90.
42. Van Holten J, Reedquist K, Sattonet-Roche P, Smeets TJ, Plater-Zyberk C, Vervoordeldonk MJ, Tak PP. Treatment with recombinant interferon-beta reduces inflammation and slows cartilage destruction in the collagen-induced arthritis model of rheumatoid arthritis. Arthritis Res Ther. 2004;6(3):R239–49.
43. Lee J, Hong EC, Jeong H, Hwang JW, Kim H, Bae EK, Ahn JK, Choi YL, Han J, Cha HS, Koh EM. A novel histone deacetylase 6-selective inhibitor suppresses synovial inflammation and joint destruction in a collagen antibody-induced arthritis mouse model. Int J Rheum Dis. 2015;18:514–23.
44. Liu Z, Zhou L, Ma X, Sun S, Qiu H, Li H, Xu J, Liu M. Inhibitory effects of tubeimoside I on synoviocytes and collagen-induced arthritis in rats. J Cell Physiol. 2018;233:8740–53.
45. Wang X, Xia S, Fu B. RNA-seq analysis of synovial fibroblasts in human rheumatoid arthritis. Mol Med Rep. 2014;10:241–7.
46. Shimizu K, Nakajima A, Sudo K, Liu Y, Mizoroki A, Ikarashi T, Horai R, Kakuta S, Watanabe T, Iwakura Y. IL-1 receptor type 2 suppresses collagen-induced arthritis by inhibiting IL-1 signal on macrophages. J Immunol. 2015;194:3156–68.
47. Joosten LA, Helsen MM, Van de Loo FA, Van den Berg WB. Anticytokine treatment of established type II collagen-induced arthritis in DBA/1 mice. A comparative study using anti-TNF alpha, anti-IL-1 alpha/beta, and IL-1Ra. Arthritis Rheum. 1996;39:797–809.
48. Weinblatt ME, Kremer JM, Bankhurst AD, Bulpitt KJ, Fleischmann RM, Fox RI, Jackson CG, Lange M, Burge DJ. A trial of etanercept, a recombinant tumor necrosis factor receptor: Fc fusion protein, in patients with rheumatoid arthritis receiving methotrexate. N Engl J Med. 1999;340:253–9.
49. Woolley DE, Evanson JM. Collagenase and its natural inhibitors in relation to the rheumatoid joint. Connect Tissue Res. 1977;5:31–5.

Publisher's Note